Migration of latent fingermarks on non-porous surfaces: observation technique and nanoscale variations

Popov, Krastio T.
Sears, V. G.
Jones, Benjamin J.

The published article is available from doi:
https://dx.doi.org/10.1016/j.forsciint.2017.02.015

Migration of latent fingermarks on non-porous surfaces: Observation technique and nanoscale variations

KT Popov[1,2,3], VG Sears[4], BJ Jones[1,2,3*]

1. Division of Science, Abertay University, Dundee, DD1 1HG, UK
2. School of Applied Sciences, University of Huddersfield, Queensgate, Huddersfield, HD1 3DH, UK
3. School of Materials, University of Manchester, Manchester, M13 9PL, UK
4. Centre for Applied Science and Technology, Home Office, St Albans, UK

* Corresponding author b.j.jones@physics.org (B.J.Jones)

Abstract

Latent fingermark morphology was examined over a period of approximately two months. Variation in topography was observed with atomic force microscopy and the expansion of the fingermark occurred in the form of the development of an intermediate area surrounding the main fingermark ridge. On an example area of a fingermark on silicon, the intermediate region exists as a uniform 4nm thick deposit; on day 1 after deposition this region extends approximately 2µm from the edge of the main ridge deposit and expands to a maximum of ~ 4µm by day 23. Simultaneously the region breaks up, the integrity is compromised by day 16, and by day 61 the area resembles a series of interconnected islands, with coverage of approximately 60%. Observation of a similar immediate area and growth with time on surfaces such as Formica was possible by monitoring the mechanical characteristics of the fingermark and surfaces though phase contrast in tapping mode AFM. The presence of this area may affect fingermark development, for example affecting the gold distribution in vacuum metal deposition. Further study of time dependence and variation with donor may enable assessment of this area to be used to evaluate the age of fingermarks.

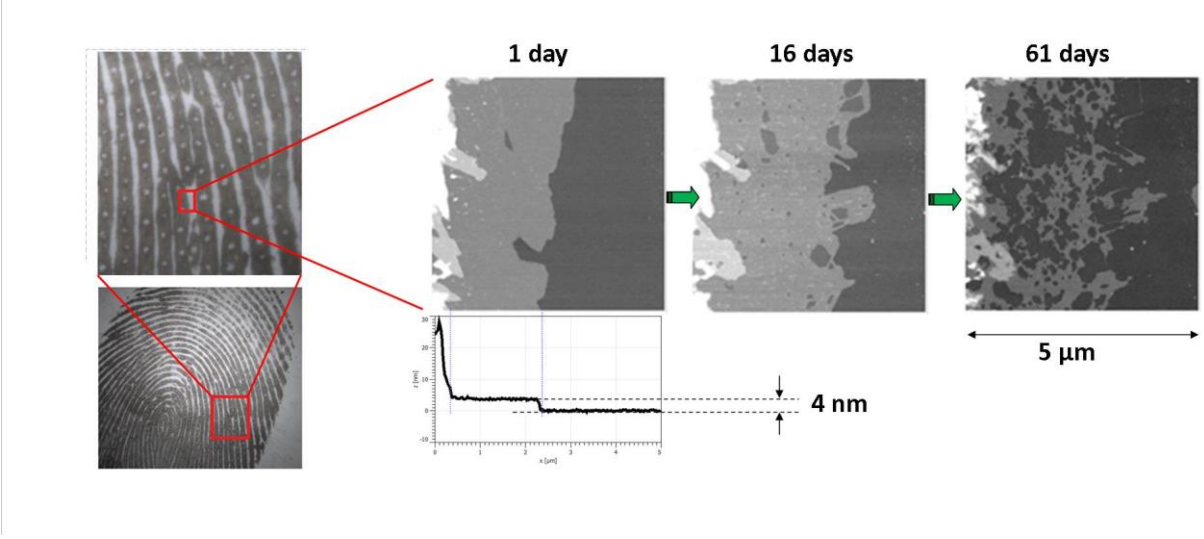

Introduction

Freshly deposited latent fingermarks consist of multiple components from eccrine and sebaceous secretions such as water, fatty acids, sterol esters, wax esters, amino acids and inorganic compounds [1,2,3,4]. Estimates of water concentration vary from less than 20% [1] to 99% [2,3]. The composition of deposited latent fingermarks may vary as a result of many factors such as: age [5,6,7,8,9,10], gender [4,6,11,12,13,14,15], race [16] and diet [11] of the donor as well as the deposition action, contact time, angle, pressure, and substrate nature which includes porosity, curvature, and texture [4,5]. Scruton et al. [17] demonstrated that the chemical composition of the material on the fingers and the substrate nature determines the initial latent fingermark ridge appearance after the deposition which could be either continuous liquid pool or droplet distribution on a thin layer of material. This and many other works refer to "latent fingerprints" [1,3,4,6,7,9-12], however the term "fingerprint" is now more commonly used for an inked deposition, and we use "fingermark" throughout this work to refer to the type of mark left at crime scenes.

The composition of latent fingermarks changes with time after deposition due to chemical, physical and biological processes such as degradation, evaporation, oxidation, and polymerization [4,5,18]. Water concentration is significantly reduced over time after deposition together with other volatile compounds [19,20,21]. The sebaceous component undergoes the most significant chemical changes with time after the deposition due to presence of saturated and unsaturated fatty acids, wax esters, squalene, cholesterol and cholesterol esters [4,5,6,11].

The deposition substrate is one of the factors which affect the way a latent fingermark alters with time after deposition [5,22]. High porosity of substrates for example: paper, cardboard and wood leads to increased penetration of the latent fingermark components into the substrate, possibly at differential rates [22,23]. Generally the eccrine components are absorbed more rapidly than the

sebaceous components. On non-porous surfaces such as many plastics, glass and metals latent fingermark components remain on the surface and are therefore more vulnerable due to environmental exposure [22,23,24]. Another possibility for time dependent effects is the corrosion process caused by ionic salts when the fingermark is deposited on metal [22,25,26]. Several factors such as surface texture, physicochemical properties, curvature, temperature, electrostatic forces and surface free energy have been also suggested to affect the latent fingermarks [5,22,27,28]. Surfaces which appear smooth to the eye often have micro or sub-micro scale roughness including topographical linear features such as ridges, valleys and scratches which affect the behaviour of the latent fingermark on the surface, as well as the development agent interaction [27,29,30].

Environmental factors such as: temperature, light exposure, humidity and air circulation also play a significant role in changing the latent fingermark composition with time. A study of Popa et al. [31] using over 800 latent fingermarks on sterile glass substrates demonstrates a decrease of the fingermark ridge width and corresponding increase in the width of valleys. When stored in an indoor environment fingermark ridge width decreased from 0.30-0.34 mm on the day after deposition to 0.24-0.28 mm after 180 days, with similar decrease for an outdoor environment. Changes in the pores were also observed such as opening of the marginal pores after 5 days. In addition to observing fingermark ridge width decrease, De Alcaraz-Fossoul et al. [32] also suggested a horizontal change in time designated “ridge drift”. The ridge drift was characterized by random changes of a single ridge original position while adjacent ridges remains unaltered which was suggested to lead to a change of the minutiae distribution. However, as the phenomenon was observed by comparing the same area of separate fresh and aged fingermarks developed with titanium dioxide powder, the observations might be a result of ridge material migration or degradation, surface texture effects or contact dynamics. Moret et al. [33] demonstrated by phase contrast microscopy the disappearance of a sebaceous loaded latent fingermark ridge pattern on polypropylene (PP) and polyvinyl chloride (PVC) from 4 days while on glass the fingermark remained visible for the maximum study period of 58 days. On PP after 4 days a barely seen ridge outline was observed while only certain droplets from

the ridges could be observed between 4 and 58 days. On PVC the ridge pattern disappearance was found to be faster than on PP resulting no visible ridge pattern from day 4 onwards. However, only sebaceous loaded latent fingermarks from only one donor were used in this study. Muramoto et al. [34] demonstrated that palmitic acid in a latent fingermark in vacuum migrates across a surface moving from ridge to ridge, a few hundred micrometres, in 4 days on silicon. This study utilized time of flight secondary ion mass spectrometry (TOF-SIMS) to image the changes between 1 and 96 hours after deposition of latent fingermarks from one donor on silicon wafers. This is a high vacuum technique which is likely to increase the mobility of material on the surface versus normal air environment. All these four studies are focused on horizontal changes of fingermark ridges while Thomas et al. [35] is focused on the height changes of latent fingermark ridges. Latent fingermark samples on microscope glass slides from each of the four donors in this study were left in six different environments for period up to three months and the thicknesses of three droplets per sample were calculated from the refractive index and the phase shift by the use of Interference microscopy. The droplet cross-section profile changes and maximum droplet thickness and lateral dimension decreases with time in various environments, and the viscosity changes with time were observed. Varying drying rate within the droplet due to chemical inhomogeneity was proposed as a possible cause for the irregular topography observed with time after the deposition. The large initial change in the topography was suggested to be related to evaporation of more volatile components. No dependence between the drying rate and the environment humidity was observed, suggesting a low water concentration at the droplet surface [35]. However the results in the study of Thomas et al. [35] are obtained by interference microscopy with limited spatial sensitivity, and more sensitive techniques such as AFM were subsequently utilised for fingermark analysis [26,36] enabling sub nanometre resolution. Watson et al. [36] investigated the possibility of using AFM for study of fresh single and overlapping latent fingermarks on microscope glass in air and liquid environment gathering information on topography and adhesion. However this study involves Contact Mode AFM which can cause damage to delicate materials such as the freshly deposited latent fingermarks.

Goddard et al. [26] used Tapping or Intermittent Mode AFM to image corrosion caused by latent fingermark deposits on polished and untreated brass substrates. Fingermarks were removed from all samples prior to examination, the AFM measurements therefore analysed the effects of the fingermark and environment on the underlying substrate material; samples exposed to flames demonstrated measureable corrosion where fingermark ridges were located.

There are many development methods used for visualizing latent fingermarks. In some cases a specific component or group of components is the target of those methods. This coupled with the chemical and topographical changes to the fingermark with time, can provide some explanation for the time-dependent variation of effectiveness of fingermark development methods.

Powder dusting is effective on fresh fingermarks, but decreases in efficacy as the marks age [37]. This is probably due to the hardening of the fingermark as a result of loss of water [38,39], oxidation and saturation of the unsaturated compounds [6,38,40,41] as well as polymerization [7]. Powder suspension development of latent marks is strongly affected by the substrate chemistry and texture [27,28] as well as the formulation of the development agent [28,42]. A surface dependent phenomenon found is the variation of particle distribution on the developed fingermark ridge where the particles appeared concentrated and further surrounded by less concentrated area which ends with highly concentrated edge, this may be related to substrate-dependent lateral changes in the fingermark following deposition.

Vacuum Metal Deposition (VMD) efficacy is also affected by aging of fingermarks, and is particularly useful for old and environmentally exposed fingermarks [43]. In its most common form, VMD is a two stage vacuum process of gold evaporation and deposition followed by evaporation and deposition of zinc. It is suggested [44] that in this process exposed gold particles located between the fingermark ridges serve as binding sites for the zinc while on the ridges the gold particles are submerged into the deposited material and cannot bind the zinc, leading to normal development with zinc between the ridges and surrounding the fingermark. However, reverse development (zinc on the ridges but not

between and not surrounding the mark) as well as empty prints (no zinc on the ridges or between them but surrounds the fingermark) and overdevelopment (zinc deposited everywhere) are also often found in practice. There are some evidence that these problematic developments are related to the substrate [45,46] although it is not clear if this is caused by direct development agent interaction with the substrate, or the effects of the surface properties on the behaviour of the deposited fingermark.

Earlier research has demonstrated the importance of micro and nano level features on both substrate [27,28,30] and development agent [29,42] in affecting the behaviour and visualization of the fingermark. This work examines latent fingermark topography on a micro and nano level and how this topography varies with time after the deposition of the mark.

Materials and methods

Substrates and fingermark samples

In order to study the variation of fingermark topography natural fingermarks were deposited on a substrate of polished (100) silicon wafer (Cascade Scientific Ltd) or Formica wafer. A total of eight donors were studied, and detailed analysis of one mark for each substrate from one donor is presented here, although all donors exhibit the effects presented and inter- and intra-donor variation will be presented in part II of this work. A silicon wafer cleaved and polished to present a (100) crystallographic plane surface was used as a model substrate. Unlike other substrates such as polished glass, metals, plastics, stones which appear flat but have some micro or nanoscale texture, the use of atomically flat silicon ensures substrate topography is not a confounding factor in the migration of fingermarks on this model surface. The surface energy of silicon was calculated using sessile drop methods with water and ethylene glycol and Owens-Wendt extrapolation as 45.0 mN/m (Polar: 24.7 mN/m and Dispersive: 20.4 mN/m). A Formica wafer was used as a forensic practice related substrate, selected as an example of substrate often found at crime scenes. The batch of Formica was provided by Home Office and has been previously characterized in an earlier work [27].

Surface texture information includes roughness measurements for this substrate: R_a (average deviation from mean line) 22.8 ± 3.5 nm, R_{max} (maximum height variation) 0.49 ± 0.1 µm, Kurtosis (peak sharpness) 6.8 ± 1.6 and Skew (symmetry) 1.0 ± 0.4. The surface energy was calculated as 33.9 mN/m (Polar: 11.1 mN/m, Dispersive: 22.8 mN/m). Behaviour of marks on other surfaces will be examined in part II of this study. Reference points were artificially added on the polished silicon and Formica surfaces to aid identification of the scanning area for repeat measurements over a series of time points.

The only instruction to the donors was to avoid hand washing for at least 30 mins prior to deposition on either polished silicon or Formica in order to produce natural fingermarks without sebaceous or eccrine loading [27,29]. The samples were left horizontally in ambient environment (variable humidity and temperature 20-25 ^{o}C) for approximately 2 months with non-airtight, translucent covering to reduce direct deposition of dust particles but to allow passing of light and air. This work was approved by relevant University Research Ethics Committee (REC), the fingermark donors gave informed consent for participation in this study and collection of fingermarks was conducted in accordance with REC guidelines.

Atomic Force Microscopy (AFM) examination of clean substrates and fingermark samples

Atomic Force Microscope (AFM) measurements were conducted at three randomly selected locations for each of the clean substrates before fingermark deposition, utilizing a Bruker Dimension Icon AFM operating in Soft Tapping mode in air and Scanasyst-AIR cantilever, with a resonant frequency of approximately 80 kHz. After fingermarks deposition AFM measurements were conducted at a range of time points. The artificially added substrate reference points were used to aid identification of the scanning area for repeat measurements over a series of time points, enabling study of the topography at the same location at each time point. The fingermark area on polished silicon was examined at 1, 8, 16, 23, 30, 44 and 61 days while the fingermark area on Formica was

examined at 1, 8, 16, 21, 44 and 69 days followed by examination of the same area after cleaning. The images presented relate to one fingermark per surface to enable comparison of time points.

Data analysis

The AFM data including height diagrams and phase maps of the clean substrates and the fingermarks on these substrates was processed by Bruker Nanoscope Analysis software applying 1st order plane fit for tilt correction. The topographic data of fingermarks on polished silicon was analysed with the same software by using a bearing analysis approach. This shows the percentage of an area with certain depth from the total area of the capture. The exported data from the histograms were used for further analysis by using peak value positions and thickness error by using half peak width approach. The surface coverage of the fingermark and the corresponding error were calculated from the exported bearing area graphic data. Section analysis was performed with Bruker Nanoscope Analysis software to demonstrate changes with time in the XY plane.

Results and Discussion

Topography changes with time after the deposition of latent fingermark on polished silicon.

The polished silicon is a nano-scale flat surface without mechanical stiffness variation as seen in figure 1 which represents 20 µm-square atomic force microscopy height and the corresponding phase maps at three randomly selected areas. Figure 2 shows 20 µm-square height maps of one area of fingermark at seven different time points, the area represents a boundary of a fingermark ridge. The main ridge deposit on the left side of the image consists of a complex suspension likely to compose of mainly water, triglycerides, fatty acids, wax esters, squalene, cholesterol, cholesterol esters, aminoacids, proteins, glucose, lactate, urea, pyruvate, and salts and [4,5,6]. The presence of a thin, uniform layer of deposited material surrounding the main ridge deposit, designated here as the "intermediate area", is observed at all time-points (Fig.2). The edge of the main ridge deposit is annotated with 'arrow 1' in figure 2a and the edge of the intermediate area is annotated with 'arrow

2’. The intermediate area spreads horizontally and then disrupts with time after the deposition (Fig.2). There are also few smaller flat areas visible in this scan size at the edge of the main ridge deposit which appear as a second intermediate area located above the large intermediate area. To better show height distribution of components of the latent fingermark and to help remove factors such as noise and adventitious surface contamination, changes in the main ridge deposit are observed through bearing analysis of the 20 x 20 µm scanned area. Figure 4 presents the bearing analysis with the maximum height of the lowest stated proportion of the surface; for example on day 1, the maximum height of the mark is 319nm, but 99.9% of the surface is below 192nm, and 85% below 18nm. The absolute percentage surface values are dependent on the proportion of bare substrate within the scan, however, this analysis allows good comparison between the different time points. When 99% of the scanned area is compared in all time points there is an initial increase in height from 96 nm at day 1 to 111 nm at day 8 and then gradual decrease to 72nm at day 61 (Fig. 4). This increase in height of mark in the initial two weeks is not observed at the lower percentiles. This represents an initial clustering of the deposit into higher globules, and then a gradual decrease as material is lost or spreads. The phase maps seen on figure 3 show the deposited material distribution on the scanned area due to the difference of the mechanical stiffness between the fingermark material and the silicon. The intermediate area is subject to horizontal spreading and subsequent disruption. In order to observe better the time dependent changes in the intermediate area a 5 x 5 µm AFM scan size was conducted at each time point in the same area (Fig. 5 and 6) located over the ridge boundary in the centre of the 20 x 20 µm scanned areas as annotated at the first scan (Fig.2a). Bearing analysis and section analysis of the topographic data were used to provide further information on the nature of the intermediate area as summarised in Figure 7. The bearing analysis shows the percentage of total area at each height within the full range and allowed calculation of the intermediate area percentage from the total scanned area (Fig. 7a) as well as the intermediate area thickness (Fig. 7c). Exported data from the histograms and the distance between the peaks allowed calculation of the thickness while the width of the peaks which characterize the uniformity allowed

calculation of the thickness variation of the intermediate area as a layer. The section analysis enabled assessment of the maximum extent of the intermediate region within the observed area (Fig. 7b). At day 1 the intermediate area in this region appears as a uniform, uninterrupted layer of deposit (Fig.5a) with thickness of 3.7 nm ± 0.7 nm (Fig.7c) and extending a maximum of 2.235 μm from the ridge edge (Fig. 7b). At day 8 (Fig. 5b) the intermediate area expands to approximately 137% of the area initially covered (Fig. 7a) and the limit increases to 3.235 μm in width (Fig. 7b) while the thickness remains at approximately 4 nm (Fig. 7c). As shown in figure 5, the expansion process is not uniform throughout the whole area. A disruption process also starts to appear after day 8 and the integrity of coverage is reduced but the area covered maintains 4nm thickness, although with increased variation over the area through development of surface texture, as shown in figure (Fig. 5c). The small flat areas of the main ridge deposits which look like a second intermediate area are also characterized by some horizontal expansion and disruption in a similar manner to the large intermediate area underneath. At day 16 (Fig. 5c) the intermediate area decreased to 128% in comparison with day 1 (Fig. 7a) while the limit expansion continues to 3.490 μm in width (Fig. 7b) but with little change to the thickness (Fig. 7c). The disruption process also continues both with increase in size of the holes and is initiated in more locations as smaller new holes appear, together causing further decrease in covered areas. The horizontal expansion and some small disruption continue in the flat second intermediate like areas of main ridge deposit. At day 30 the disruption process in the intermediate area starts to dominate over the limit expansion (Fig. 5e). Many holes with various sizes in the intermediate area and some clearly visible disruptions of the areas similar to a second intermediate area are observable at this time point. All of these caused further decrease of the intermediate area to 103% (Fig.7a). The thickness of the deposit in the intermediate area remains again approximately 4 nm (Fig. 7c). At day 44 the intermediate area is significantly disrupted and is more accurately described as an area of random shaped, loosely connected islands of deposit (Fig. 5f), each with approximate thickness of 4 nm (Fig. 7c) and total coverage of approximately 71% (Fig. 7a) of the initial intermediate area at day 1, although the limit of this region is increased to 3.961 μm

from 2.235 µm (Fig. 7b). Further disruption of the areas similar to a second intermediate area continues to be observed in the main ridge deposit. At day 61 (Fig. 5g) there are further small disruption changes in the 4 nm thick (Fig. 7c) random shaped island appearance of the intermediate area which covers approximately 69% of the initial intermediate area at day 1 (Fig. 7a) as well as some disruption in the second intermediate layer like structures (Fig. 5g). The mechanical stiffness difference between the deposited material and the silicon substrate appears to decrease with time after the deposition (Fig. 6). It is reasonable that the intermediate area is formed by components with lower viscosities which spread from the main ridge deposit and then may evaporate or degrade chemically with time after the deposition. Based on composition information from Cadd's review and earlier studies [4,5,6,11] possible candidates are the water, and sebaceous components such as some of the fatty acids and triglycerides. Unsaturated fatty acids and the triglycerides built from them tend to be in liquid form at the room temperature of the experiment based on the melting points of the purified compounds. The aminoacids, proteins, glucose, lactate, urea and salts found in latent fingermarks [4,5,6] are solid in purified state. The inorganic compounds are relatively stable while the aminoacids, the proteins and urea decrease but still remain detectable [5]. Mong et al. [38] suggests that of 85% of the fingermark's weight is lost after two weeks, and suggests this is probably due to water loss. However, analysis by Kent in 2016 [1] indicates that high water content figures [2,3,38] are based on the eccrine sweat composition instead of the fingermark composition after the deposition. This analysis, coupled with Thomas et al. [35] who show little variation in degradation of fingermarks with humidity, suggests a more complex solution is needed. Our results show changes of the intermediate area up to two months after deposition. This time frame suggests that fatty acids are better candidates for the composition of the layer. An earlier study using GCMS to examine changes of the lipid composition with time [40] suggested that the short chain fatty acids concentration increase in the first 15 days due to degradation of the longer chain fatty acids – C14 concentration initially increases in the first 20 days followed by a decrease down to original or lower levels. Shortening the hydrocarbon chains of the fatty acids to octanoic (C8) and nonanoic (C9) acids

which are found in greater concentration in aged fingermarks and are further subject of break down and evaporation was discussed in the US Department of Justice Fingerprint Sourcebook [3]. These fatty acids are in liquid form in the temperature range of this experiment and could migrate easily. The liquid fatty acids concentration could be also increased by hydrolysis of triglycerides which delivers a mixture of saturated and unsaturated fatty acids [47]. Some of the low weight degradation products of squalene such as acetone [38,41] could serve as strong solvents for the solid components which can cause further liquidation of the ridge deposit and easier migration on the surface. It is also important to notice the hydrophilic nature of this surface which can cause significant horizontal spreading of liquid fatty acids. On the other hand unsaturated compounds such as unsaturated fatty acids and squalene tend to form oxidized solid products such as hydroperoxides or epoxides. Polymerization of unsaturated compounds by carbon-carbon bonds formation can also create waxy solid [38,40]. However the lower molecular weight and unsaturated compound migration hypothesis needs high resolution chemical analysis in order to be confirmed.

A recent study demonstrated that fingermark material in vacuum migrates across a surface - moving from ridge to ridge, a few hundred micrometres, in four days [34]. However, this study utilizes time of flight secondary ion mass spectrometry (TOF-SIMS) to image the fingermark changes. This is a high vacuum technique which is likely to increase the mobility of material on the surface and may not be directly applicable to migration of the mark components in air. The component shown to migrate in the ToF-SIMS study, palmitic acid, is solid at room temperature and pressure and whilst may be a component of the intermediate layer along with unsaturated or lower molecular weight products, is unlikely to fully explain the development of intermediate area in ambient conditions.

A previous study on development of marks with powder suspension on polymer substrates [27] shows different behaviour of the developing agent at the edge of the ridges. One of the possible explanations could be the presence of intermediate area. Migration of material from the fingermark ridge has also been postulated as the cause of the variation seen in VMD development on different polymers [45,46].

Topography changes with time after the deposition of latent fingermark deposited on Formica.

The polished silicon used in the previous section is a homogeneous, nano-scale flat, nonporous surface enabling its use as a model surface in the study of latent fingermark migration across the surface. However, this material is unlikely to be found on crime scenes and therefore further study with forensically relevant substrate Formica was conducted. Figure 8 shows 20 µm-square atomic force microscopy height and the corresponding phase maps at three randomly selected areas of clean Formica surface. The phase maps show no mechanical stiffness variation at the clean Formica surface (Fig. 8d, 8e and 8f) and the surface is consistent with previous study [27].

The AFM examinations of a latent fingermark on Formica were conducted at the same location at different time points after the deposition. Figure 9a-9h shows 20 µm-square atomic force microscopy height and phase maps of one area of fingermark at four different time points as well as the cleaned surface of the same area (Fig. 9i and 9j). This area represents a boundary of a fingermark ridge and the underlying structure shown on the cleaned substrate image. As in the fingermark on the silicon model surface the main ridge deposit can be observed on the left side of the image. At day 1 a clearly defined fingermark ridge is observed on the left side of the image despite the substrate roughness visible on the right side (Fig. 9a). This boundary was observed better on the phase map which characterizes the mechanical stiffness variation of the scanned area and enables distinction of the fingermark deposit due to the difference in mechanical properties between the fingermark and the substrate (Fig. 9b). A week later at day 8 there is a change of the ridge topography which could be easily observed as well as horizontal migration of material reaching approximately 5 µm distance from the ridge (Fig. 9c). The horizontal migration was again observed better on the phase map (Fig. 9d) due to the different stiffness of the deposited material versus the Formica. It appeared that the horizontal spreading of the ridge material became limited by major substrate ridge which could be observed on the right side of the scanned area annotated with arrow (Fig. 9c). There were also signs of horizontal migration from the opposite direction probably from the next fingermark ridge. At day

16 faster horizontal migration through a scratch could be observed even better on the phase image despite the large offset of the scale (Fig.9f). Significant concentration of horizontally migrated material through the scratch could be seen on the same phase map. Possible migration from another ridge should be also considered. At day 21 further migration could be observed again better on the phase map (Fig.9h) resulting larger area of the substrate covered with ridge material. After all time points the sample was cleaned again and the clean Formica substrate was examined at the same area providing us with the information for the substrate roughness (Fig.9i) and substrate stiffness variation (Fig.9j) below the fingermark. It appeared that the substrate at the scanned area had few major ridges as well as significant scratch which affected the horizontal migration of the latent fingermark deposit. The scanned area appeared relatively homogeneous in stiffness which allowed us to observe better the horizontal migration of the fingermark deposit.

The increased deposit migration speed on Formica could be a result of the scratches or scratch-like substrate morphology on the surface. There are also examples that suggest such increased migration through scratches or sharp valleys based on local overdevelopment in such structures [27,30]. Another possible cause of the rate of deposit migration is aligned to suggestions by workers such as Bobev [22] and findings such as that in Bacon et al. [28] who proposed the possible causes for the variation of latent fingermark behaviour on materials includes surface energy considerations, reflected here in the difference in the surface energy of Formica compared to that of silicon.

The initiation and development of a nanoscale intermediate area spreading out from the ridges as the marks age is in contrast to the observations of ridge contraction with time observed at micro and macroscale [31-33]. However, the presence and spread of the intermediate area could affect the fingermark visualization, for example through powder adhesion or gold particle distribution in VMD, as well as the interpretation of marks by edgeoscopy. A fatty acid layer of similar thickness to the intermediate area observed here has been found to inhibit completely the second metal deposition in VMD [35]. The surface and donor dependent variation in extent and speed of development of this

intermediate area could be the cause of the surface dependent behaviour of VMD, such as the empty prints on specific polymers earlier observed [45]. However, the same variation may lead to difficulties in utilizing the fingermark spreading phenomenon to determine a forensic timeline.

Conclusions

Nano and micro scale topography of latent fingermarks were observed to change with time over a two-month period after deposition. Atomic force microscopy measurements showed a decrease in the height of the fingermark ridge and a horizontal migration of the components, on both a model silicon surface and a forensically relevant Formica substrate. The AFM highlights a relatively uniform layer of deposit of approximate thickness 4nm, designated “intermediate area”, surrounding the main fingermark ridge. On the example mark on model silicon substrate this intermediate area is visible for a width of approximately 2 µm on the first day after fingermark deposition, and expands to approximately 4 µm in width within the next three weeks, with the limit remaining constant thereafter. Similar to the limit the intermediate area coverage from the total scanned area expands to 137% of initial coverage reaching a maximum at day 8 but it is followed by disruption and decrease in the percentage coverage to an equivalent of 69% of initial area after 2 months. The roughness of polymer samples exceed the thickness of the intermediate area making direct observation of the intermediate area topography variation impossible, except where surface structures cause capillary-type migration. However, similar intermediate areas can be observed on Formica using tapping mode AFM to observe mechanical properties of the fingermark and substrate. Initial spread of the intermediate area on Formica in this instance is up to 5 µm and is limited by the substrate topography. Rate of spread of material is uneven and occurs generally faster in comparison to polished nano-flat silicon especially where scratches are present on Formica surface. Samples exhibit intermediate areas of differing sizes, and the behaviour of the deposit is thought to be affected by its

components and the substrate texture and surface energy. Analysis of the spread of the fingermark may provide added intelligence concerning the mark donor. Despite the thinness of spreading material, such changes in latent fingermark topography with time may alter the developing agent distribution, such as the efficacy of VMD development which is linked to nanoparticulate gold deposition.

Acknowledgements:

This project was partially funded through the UK Home Office 7200304. We are pleased to thank Mrs Katie Addinall, Professor Liam Blunt, Mr Jack Cammidge, and Dr Chris Dawson for technical support.

Author Contributions:

KTP and BJJ designed the experiments as part of a project designed by BJJ and VGS. KTP conducted the AFM measurements which were analysed and interpreted by KTP and BJJ, with regular input from VGS. KTP and BJJ wrote the manuscript. KTP, VGS and BJJ revised and approved the manuscript.

References:

1. Kent, T., Water Content of Latent Fingerprints–Dispelling the Myth, *Forensic Sci. Int.* **266**, 134–138 (2016).
2. Llewellyn, P. Jr. & Dinkins, L. New use for an old friend. J. Forensic Identif. 42, 498–503 (1995).
3. Yamashita, B. & French, M. Latent print development, in: Fingerprint Sourcebook, NCJ 225320, US Department of Justice, Washington, (2011).
4. Cadd, S., Islam, M., Manson, P. & Bleay S. Fingerprint composition and aging: A literature review. *Sci Justice.* **55**, 219–238 (2015).
5. Girod, A., Ramotowski, R. & Weyermann, C. Composition of fingermark residue: a qualitative and quantitative review. *Forensic Sci. Int.* **223**, 10–24 (2012).
6. Ramotowski, R. Composition of latent print residue, in: Lee, H.C. & Gaensslen, R.E. (Eds.), *Advances in Fingerprint Technology.* **2nd ed.CRC Press, London**, 63–104 (2001).
7. Mong, G., Walter, S., Cantu, T. & Ramotowski, R. The chemistry of latent prints from children and adults. *Fingerprint Whorld.* **27**, 66–69 (2001).

8. Ramasastry, P., Downing, D.T., Pochi, P.E. & Strauss, J.S. Chemical composition of human skin surface lipids from birth to puberty. *J. Investig. Dermatol.* **54**, 139–144 (1970).
9. Buchanan, M., Asano, K. & Bohanon, A. Chemical characterization of fingerprints from adults and children, SPIE (International Society for Optical Engineering). *Forensic Evid. Anal. Crime Scene Investig.* **2941**, 89–95 (1997).
10. Antoine, K., Mortazavi, S., Miller, A. & Miller, L. Chemical differences are observed in children's versus adults' latent fingerprints as a function of time. *J. Forensic Sci.* **55**, 513–518 (2010).
11. Croxton, R., Baron, M., Butler, D., Kent, T. & Sears, V. Variation in amino acid and lipid composition in latent fingerprints. *Forensic Sci. Int.* **199**, 93–102 (2010).
12. Asano, K., Bayne, C., Horsman, K. & Buchanan, M. Chemical composition of fingerprints for gender determination. *J. Forensic Sci.* **47**, 805–807 (2002).
13. Penn, D., Oberzaucher, E., Grammer, K., Fischer, G., Soini, H., Wiesler, D., Novotny, M., Dixon, S., Xu, Y. & Brereton, R. Individual and gender fingerprints in human body odour. *J. R. Soc.* Interface. **4**, 331–340 (2007).
14. de Puit, M., Ismail, M. & Xu, X. LCMS analysis of fingerprints, the amino acid profile of 20 donors. *J. Forensic Sci.* **59**, 367–370 (2013).
15. Jacobsen, E., Billings, J.K., Frantz, R.A., Kinney C.K., Stewart, M.E. & Downing D.T. Age-related changes in sebaceous wax ester secretion rates in men and women. *J. Investig. Dermatol.* **85**, 483–485 (1985).
16. Michalski, S., Shaler, R. & Dorman F.L. The evaluation of fatty acid ratios in latent fingermarks by gas chromatography/mass spectrometry (GC/MS) analysis. *J. Forensic Sci.* **58**, S215–S220 (2013).
17. Scruton, B., Robins, B. W. & Blot, B. H. The deposition of fingerprint films. *J. Phys. D: Appl. Phys.* **8,** 714-723 (1975).
18. Weyermann, C. & Ribaux, O. Situating forensic traces in time. *Sci. Justice.* **52**, 68–75 (2012).
19. Thomas, G.L. The resistivity of fingerprints. *J. Forensic Sci. Soc.* **15**, 133–135 (1975).
20. Wargacki, S., Lewis, L. & Dadmun, M. Enhancing the quality of aged latent fingerprints developed by superglue fuming: loss and replenishment of initiator. *J. Forensic Sci.* **53**, 1138–1144 (2008).
21. Sodhi, G. & Kuar, J. Powder method for detecting latent fingerprints: a review. *Forensic Sci. Int.* **120**, 172–176 (2001).
22. Bobev, K. Fingerprints and factors affecting their conditions. *J. Forensic Identif.* **45**, 176–183 (1995).
23. Almog, J., Azoury, M., Elmaliah, Y., Berenstein, L. & Zaban, A. Fingerprints' third dimension: the depth and shape of fingerprints penetration into paper — cross section examination by fluorescence microscopy. *J. Forensic Sci.* **49**, 981–985 (2004).
24. Siegel, J. & Saukko, P. Encyclopedia of Forensic Sciences. *2nd ed. Academic Press, London.* (2012).
25. Bond, J. Visualization of latent fingerprint corrosion of metallic surfaces. *J. Forensic Sci.* **53**, 812–822 (2008).
26. Goddard, A.J., Hillman, A.R. & Bond, J.W., High resolution imaging of latent fingerprints by localized corrosion on brass surfaces, J Forensic Sci. 55, 58-65 (2010).
27. Jones, B.J., Downham, R. & Sears, V.G. Effect of substrate surface topography on forensic development of latent fingerprints with iron oxide powder suspension. Surf. Interface Anal. 42, 438–442 (2010).
28. Bacon, S.R., Ojeda, J.J., Downham, R., Sears, V.G. & Jones, B.J. The effects of polymer pigmentation on fingermark development techniques. J. Forensic Sci. 58, 1486–1494 (2013).
29. Jones, B.J., Downham, R. & Sears, V.G. Nanoscale analysis of the interaction between cyanoacrylate and vacuum metal deposition in the development of latent fingermarks on low-density polyethylene. *J. Forensic Sci.* **57**, 196-200 (2012).

30. Jones, B.J., Bacon, S.R., Downham, R. & Sears, V.G. Interactions between latent fingerprints, surfaces and fingerprint development techniques. *Fingerprint Whorld.* **37**, 130-131 (2011).
31. Popa, G., Potorac, R. & Preda, N. Method for fingerprints age determination. *Rom. J. Legal Med.* **18**, 149–154 (2010).
32. De Alcaraz-Fossoul, J., Roberts, K.A., Feixat, C.B., Hogrebe, G.G. & Badia, M.G., Fingermark ridge drift, *Forensic Sci Int.* **258**, 26-31 (2016).
33. Moret S., Spindler X., Lennard C. & Roux C., Microscopic examination of fingermark residues: Opportunities for fundamental studies, *Forensic Sci. Int.* **255**, 28–37 (2015).
34. Muramoto, S. & Sisco, E. Strategies for potential age dating of fingerprints through the diffusion of sebum molecules on a nonporous surface analyzed using time-of-flight secondary ion mass spectrometry. *Anal. Chem.* **87**, 8035−8038 (2015).
35. Thomas G & Reynoldson T, Some observations on fingerprint deposits, *J. Phys. D: Appl. Phys.* **8**, 724-729 (1975).
36. Watson, G.S. & Watson, J.A., Potential applications of scanning probe microscopy in forensic science, *Journal of Physics: Conference Series* **61**, 1251–1255 (2007).
37. Champod, C., Lennard, C., Margot, P. & Stoilovic, M. Fingerprint powders, in *Fingerprints and Other Ridge Skin Impressions.* **CRC Press, Boca Raton**, 136-138 (2004)
38. Mong, G., Petersen, C. & Clauss, T. Advanced fingerprint analysis project: Fingerprint constituents. *Pacific Northwest National Laboratory Technical Report* (1999).
39. Bright, N.J., Willson, T.R., Driscoll, D.J., Reddy, S.M., Webb, R.P., Bleay, S., Ward, N.I., Kirkby, K.J. & Bailey, M.J. Chemical changes exhibited by latent fingerprints after exposure to vacuum conditions. *Forensic Sci. Int.* **230**, 81–86 (2013).
40. Archer, N., Charles, Y., Elliott, J. & Jickells, S. Changes in the lipid composition of latent fingerprint residue with time after deposition on a surface. *Forensic Sci. Int.* **154**, 224–239 (2005).
41. Mountfort, K.A., Bronstein, H., Archer, N. & Jickells, S.M. Identification of oxidation products of squalene in solution and in latent fingerprints by ESI-MS and LC/APCI-MS. *Anal. Chem.* **79**, 2650–2657 (2007).
42. Jones, B.J., Reynolds, A.J., Richardson, M. & Sears, V.G. Nano-scale composition of commercial white powders for development of latent fingerprints on adhesives. *Sci. Justice.* **50**, 150-155 (2010).
43. Theys, P., Turgis, Y., Lepareux, A., Chevet, G. & Ceccaldi, P. New technique for bringing out latent fingerprints on paper: Vacuum metallisation. *Int. Crim. Police Rev.* **217**, 106-108 (1968).
44. Robinson, C.J. The effects of a glow discharge on the nucleation characteristics of gold on polymer substrates. *Thin Solid Films.* **57**, 285–289 (1979).
45. Jones, N., Mansour, D., Stoilovic, M., Lennard, C. & Roux, C. The influence of polymer type, print donor and age on the quality of fingerprints developed on plastic substrates using vacuum metal deposition. *Forensic Sci. Int.* **124**, 167-177 (2001).
46. Jones, N., Stoilovic, M., Lennard, C. & Roux, C. Vacuum metal deposition: factors affecting normal and reverse development of latent fingerprints on polyethylene substrates. *Forensic Sci. Int.* **115**, 73-88 (2001).
47. Srivastava, A. & Prasad, R. Triglycerides-based diesel fuels. *Renew. Sust. Energ. Rev.* **4**, 111–133 (2000).

Figures:

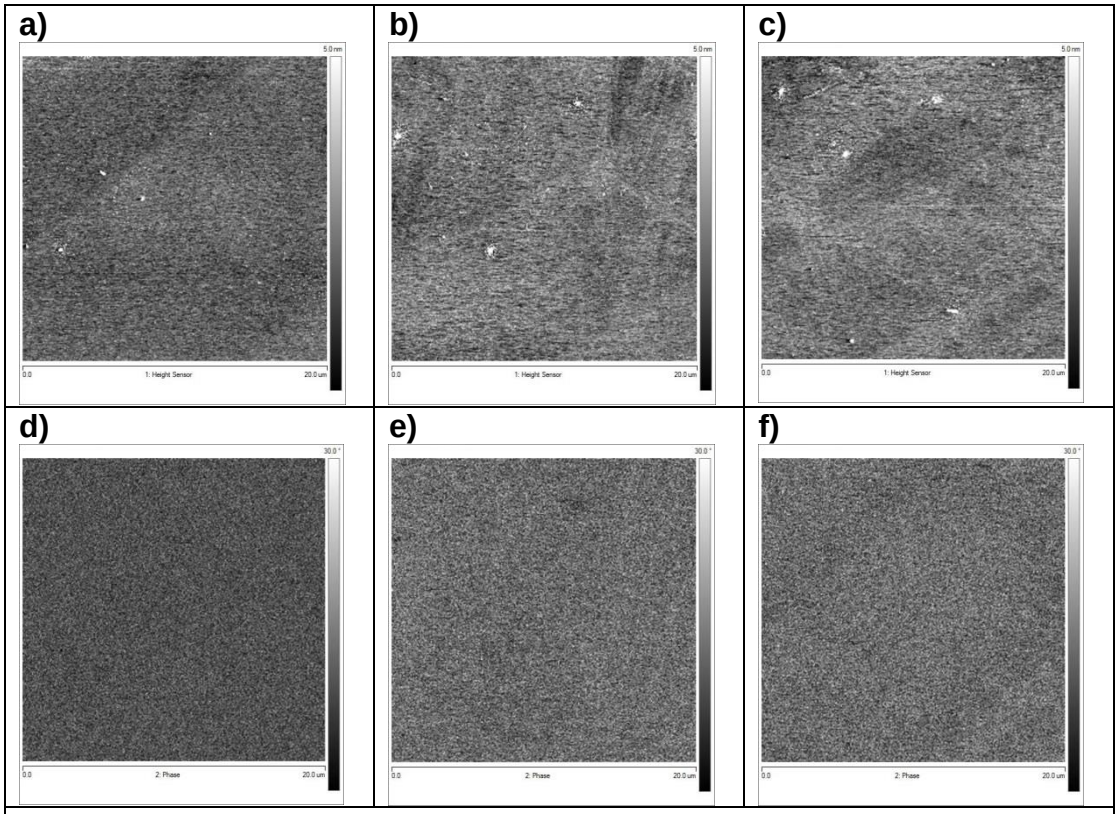

Figure 1. Clean polished silicon wafer at 20 x 20 µm scan size. Topography at 3 random locations: a), b), c) and phase pictures at the same locations: d), e), f). The grey scale on the right of each topography picture is 5 nm where 0 nm is black and 5 nm or higher is white. The grey scale on the right of each phase picture is 30 ^{o}.

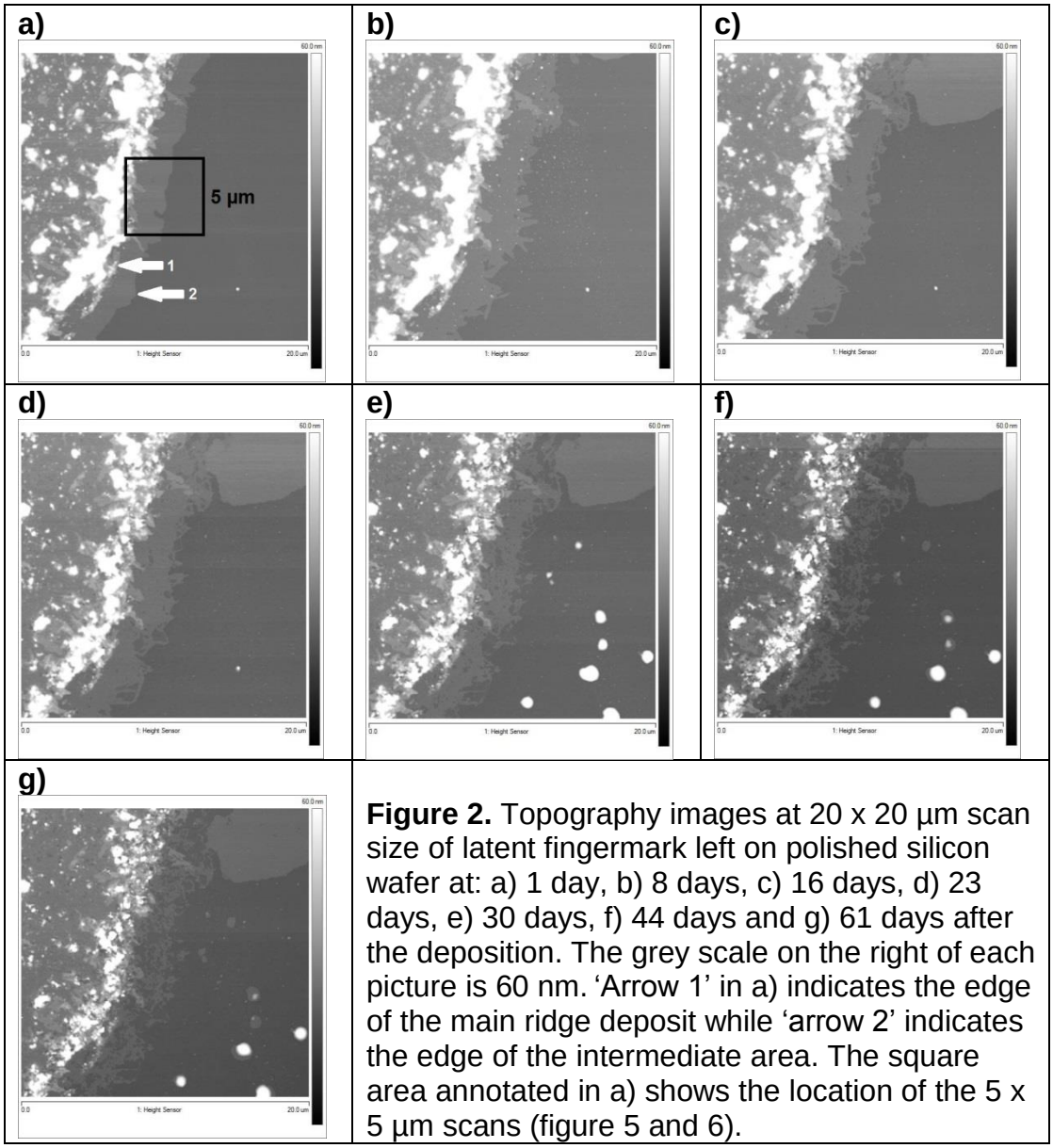

Figure 2. Topography images at 20 x 20 µm scan size of latent fingermark left on polished silicon wafer at: a) 1 day, b) 8 days, c) 16 days, d) 23 days, e) 30 days, f) 44 days and g) 61 days after the deposition. The grey scale on the right of each picture is 60 nm. 'Arrow 1' in a) indicates the edge of the main ridge deposit while 'arrow 2' indicates the edge of the intermediate area. The square area annotated in a) shows the location of the 5 x 5 µm scans (figure 5 and 6).

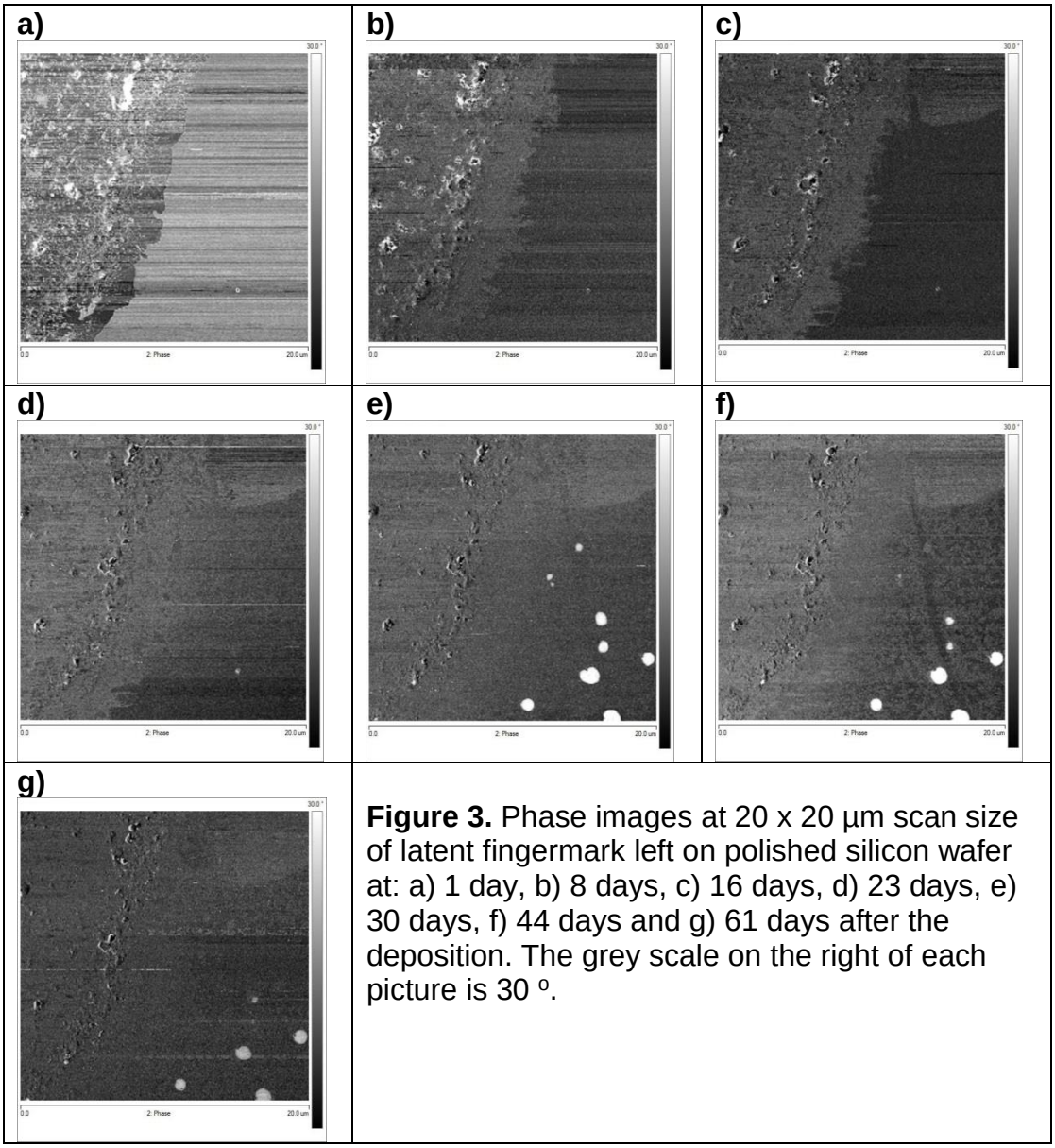

Figure 3. Phase images at 20 x 20 µm scan size of latent fingermark left on polished silicon wafer at: a) 1 day, b) 8 days, c) 16 days, d) 23 days, e) 30 days, f) 44 days and g) 61 days after the deposition. The grey scale on the right of each picture is 30 º.

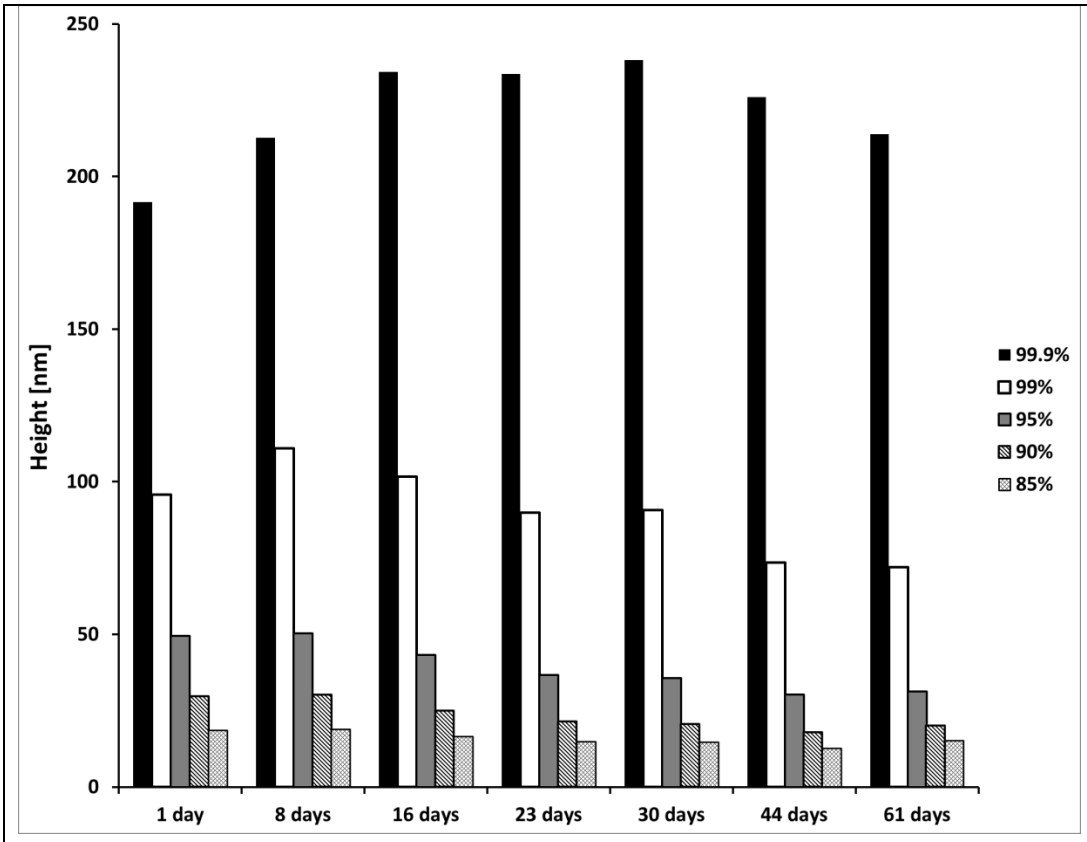

Figure 4. Height changes with time at 20 x 20 µm scan size of latent fingermark on polished silicon wafer based on the bearing analysis.

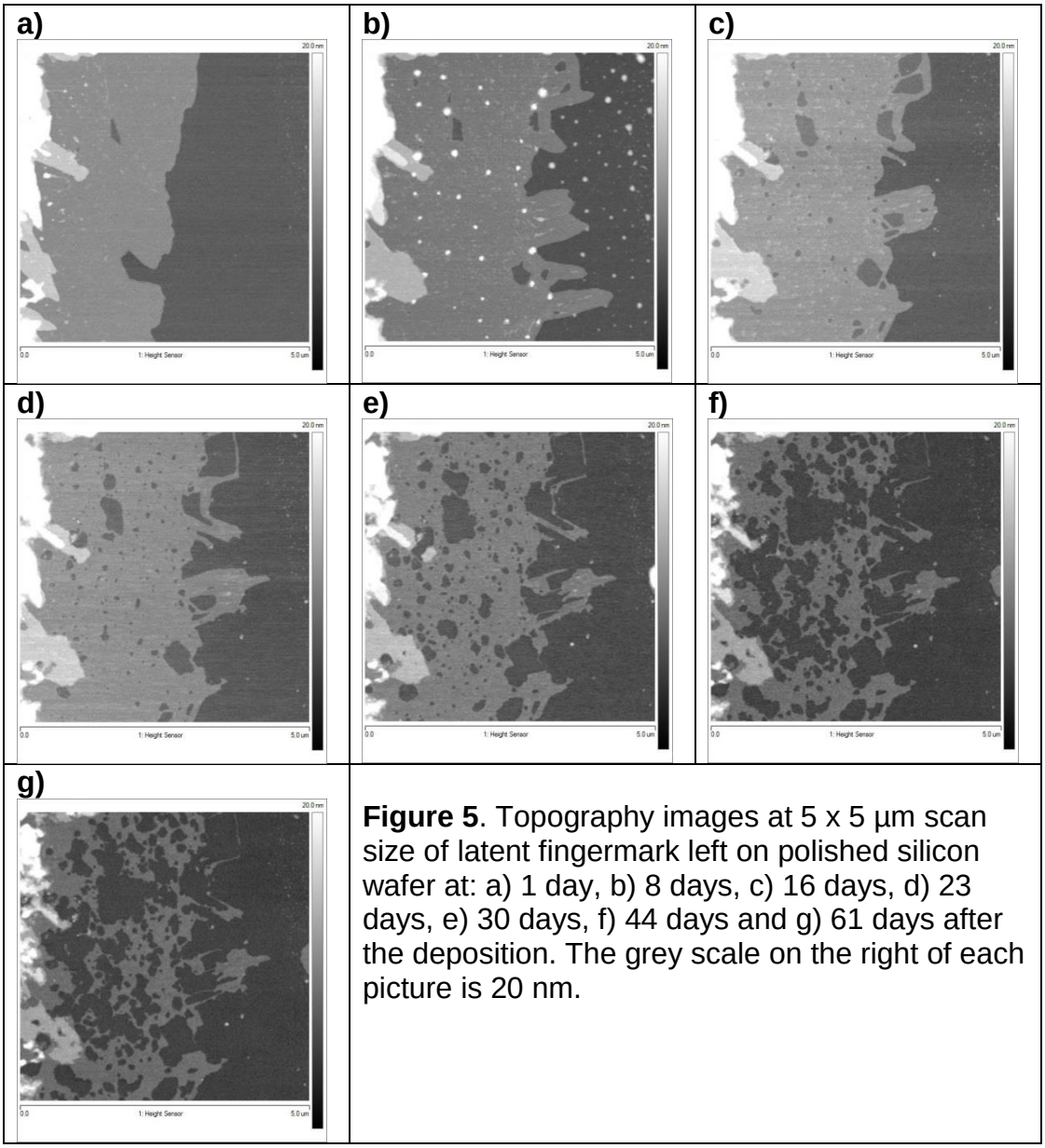

Figure 5. Topography images at 5 x 5 µm scan size of latent fingermark left on polished silicon wafer at: a) 1 day, b) 8 days, c) 16 days, d) 23 days, e) 30 days, f) 44 days and g) 61 days after the deposition. The grey scale on the right of each picture is 20 nm.

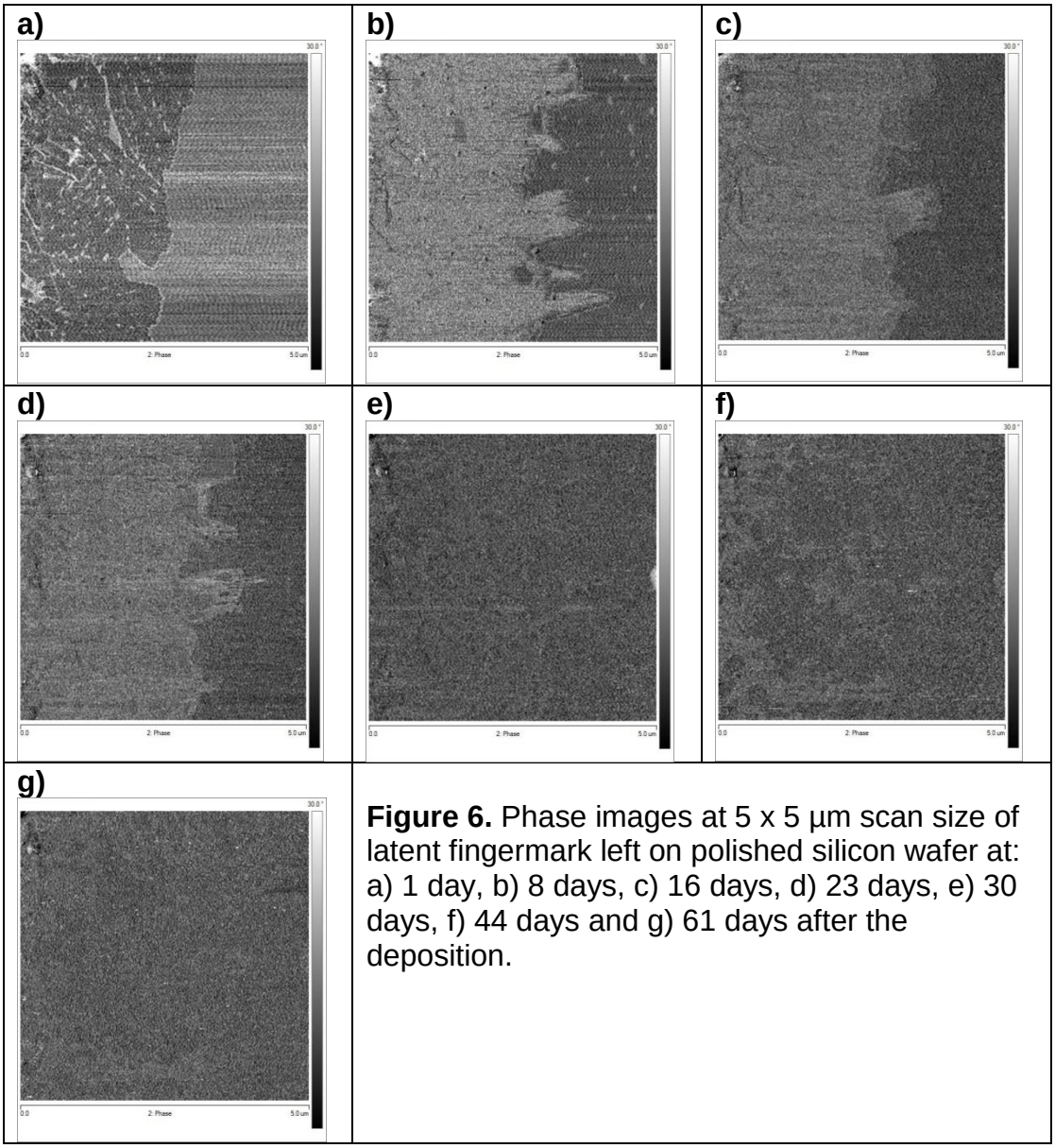

Figure 6. Phase images at 5 x 5 µm scan size of latent fingermark left on polished silicon wafer at: a) 1 day, b) 8 days, c) 16 days, d) 23 days, e) 30 days, f) 44 days and g) 61 days after the deposition.

a)

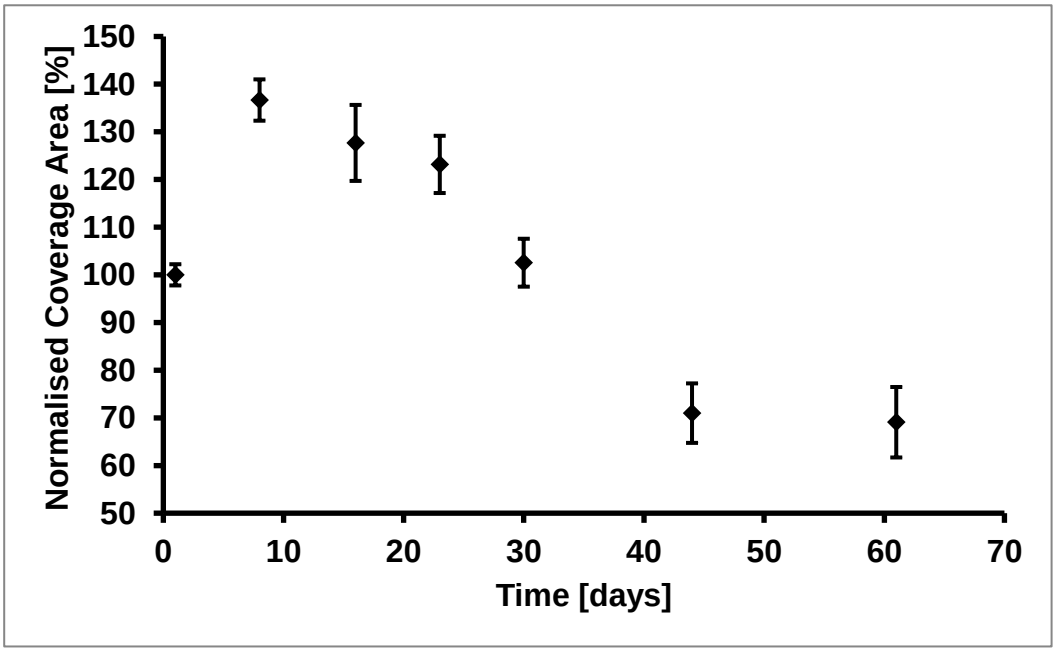
Normalised Coverage Area [%]
150
140
130
120
110
100
90
80
70
60
50
0
10
20
30
40
50
60
70
Time [days]

b)

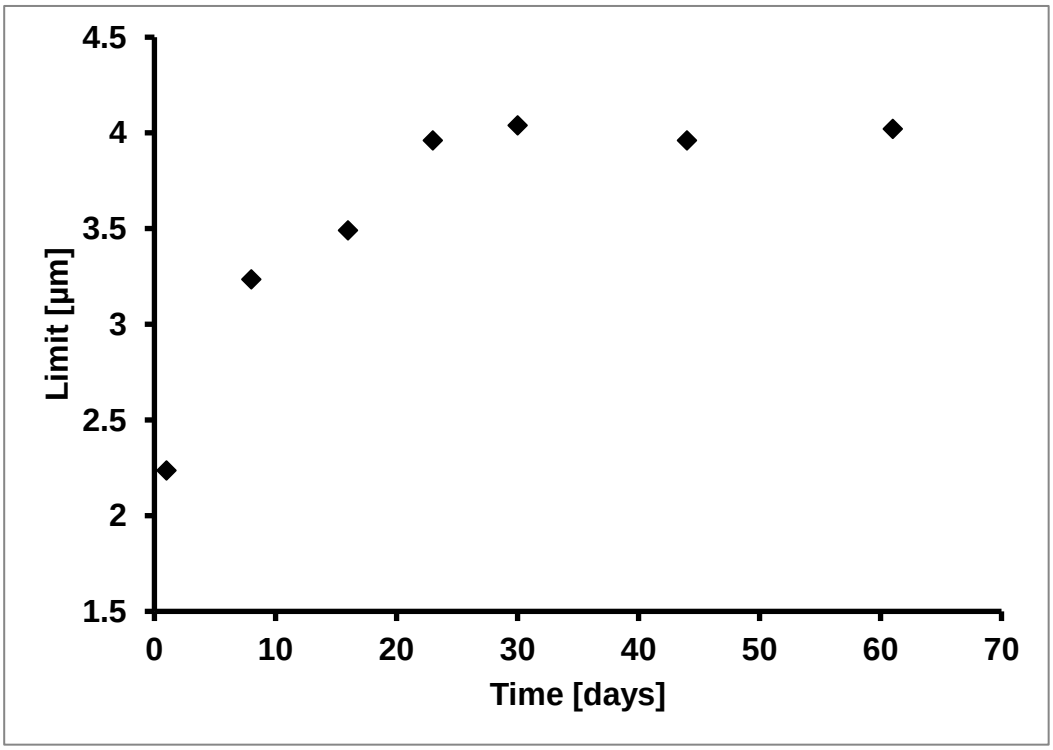
Limit [µm]
4.5
4
3.5
3
2.5
2
1.5
0
10
20
30
40
50
60
70
Time [days]

c)

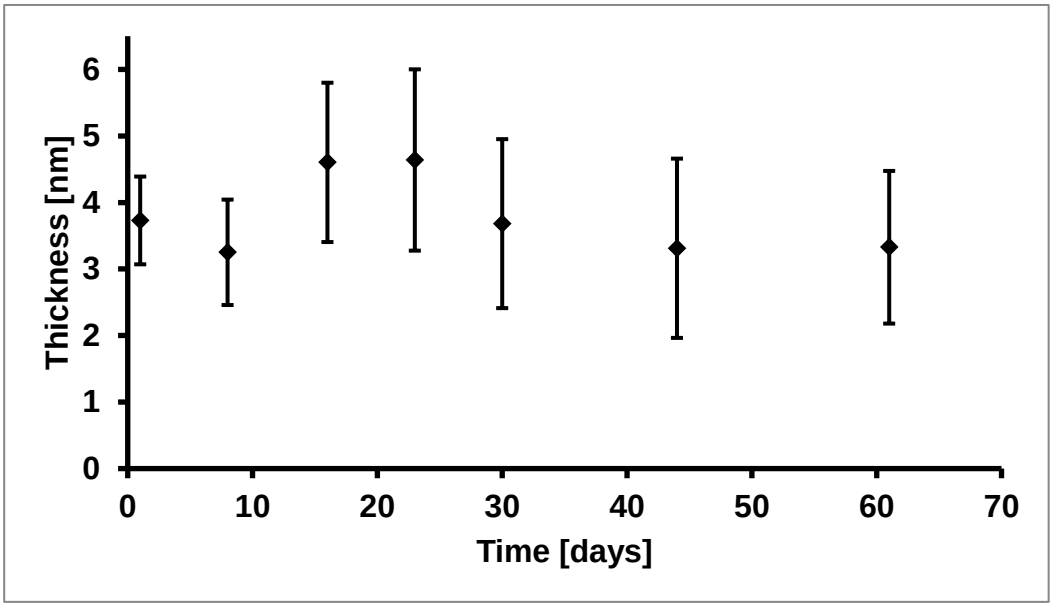

Figure 7. **a)** Normalised intermediate area coverage [%] from the 25 μm^2 scanned area (5 x 5 µm), **b)** Intermediate area limit [µm] by section and **c)** Intermediate area thickness and uniformity [nm]

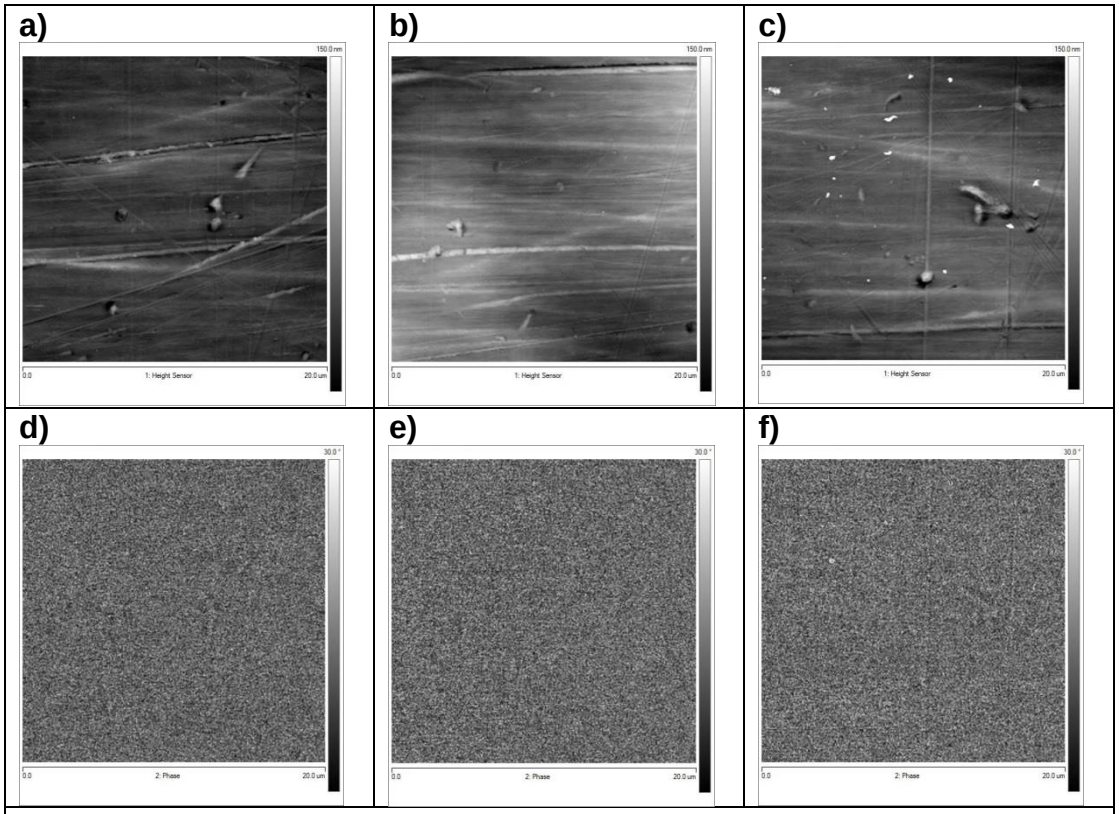

Figure 8. Clean Formica wafer at 20 x 20 µm scan size. Topography at 3 random locations: a), b), c) and phase images at the same locations: d), e), f). The grey scale on the right of each topography picture is 150 nm.

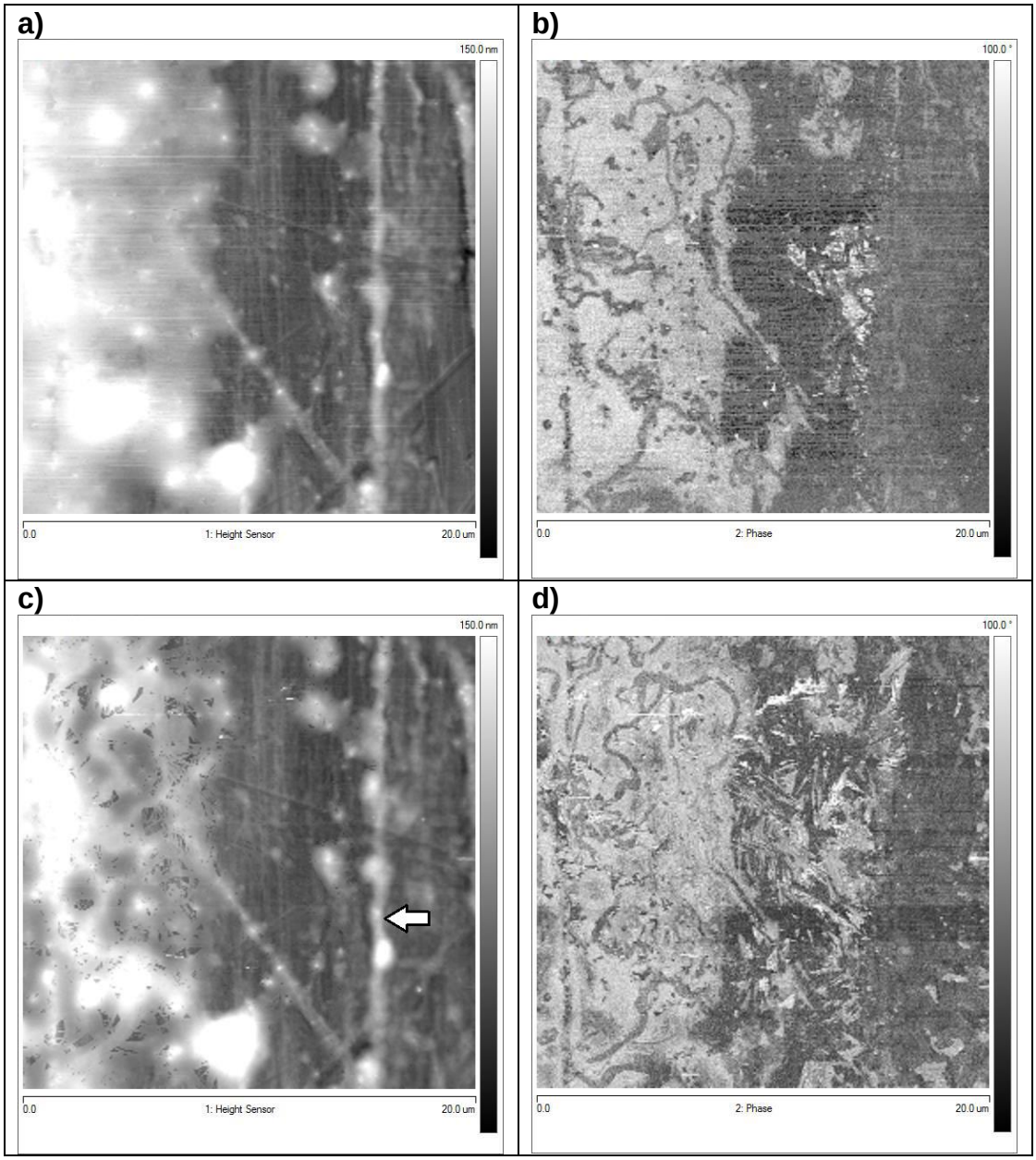
a)
150.0 nm
0.0
1: Height Sensor
20.0 um
b)
100.0 °
0.0
2: Phase
20.0 um
c)
150.0 nm
0.0
1: Height Sensor
20.0 um
d)
100.0 °
0.0
2: Phase
20.0 um

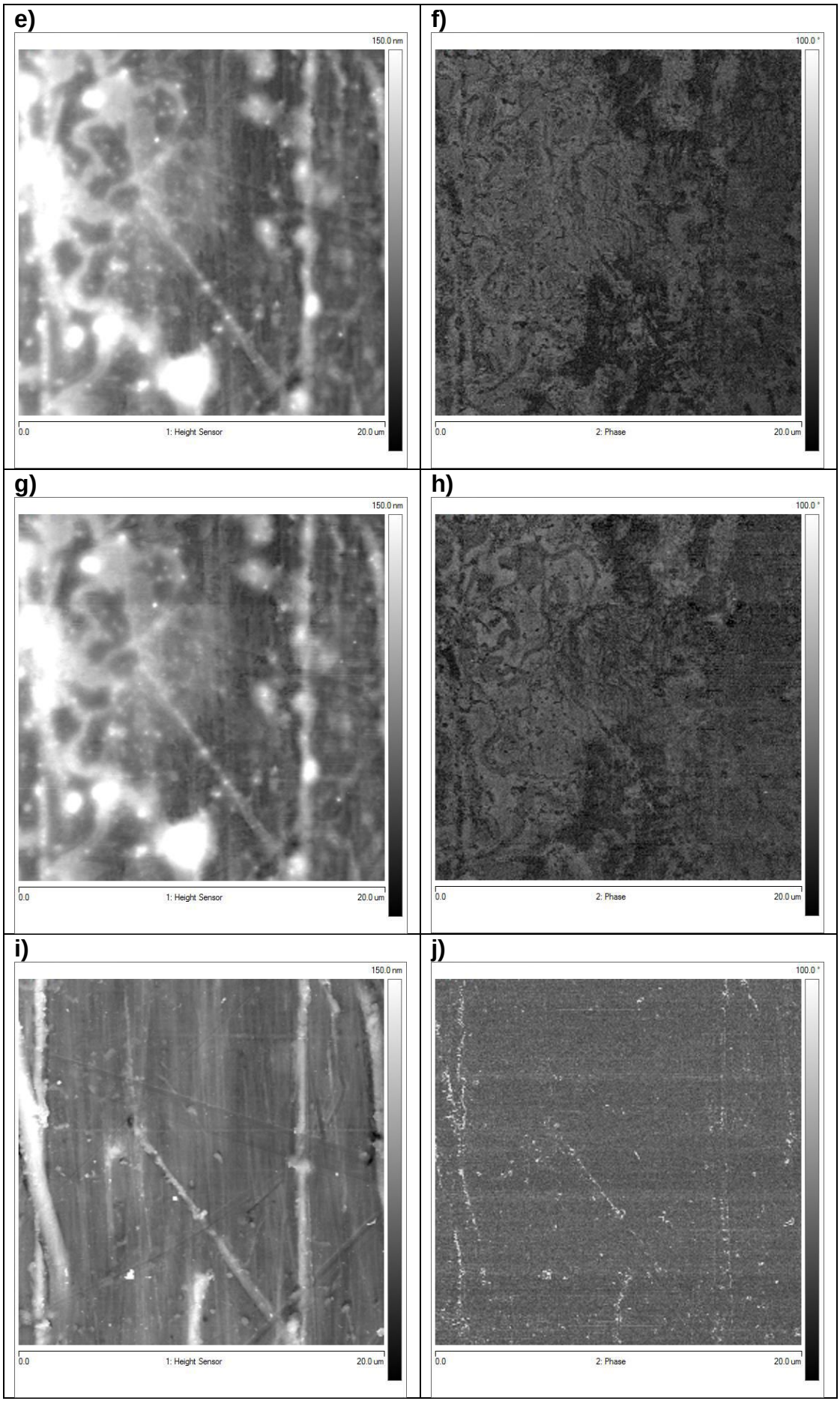
e)
150.0 nm
0.0
1: Height Sensor
20.0 um
f)
100.0 °
0.0
2: Phase
20.0 um
g)
150.0 nm
0.0
1: Height Sensor
20.0 um
h)
100.0 °
0.0
2: Phase
20.0 um
i)
150.0 nm
0.0
1: Height Sensor
20.0 um
j)
100.0 °
0.0
2: Phase
20.0 um

Figure 9. Topography and phase images at 20 x 20 μm scan size of latent fingermark ridge boundary on Formica substrate at different time points after the deposition: a) 1 day topography, b) 1 day phase, c) 8 days topography, d) 8 days phase, e) 16 days topography, f) 16 days phase, g) 21 days topography, h) 21 days phase as well as the topography i) and phase j) images of the cleaned Formica at the same area. The images represent the topography: a), c), e), g), i) with scale 0-150 nm and phase: b), d), f), h), j) .